Structural control energy of resting-state functional brain states reveals inefficient brain dynamics in psychosis vulnerability.

Short title: Control of functional brain states

Daniela Zöller[a,b,c], Corrado Sandini[c], Marie Schaer[c], Stephan Eliez[c], Danielle S. Bassett[d,e,f,g,h], Dimitri Van De Ville[a,b]

[a] *Medical Image Processing Laboratory, Institute of Bioengineering, École Polytechnique Fédérale de Lausanne (EPFL), Lausanne, Switzerland*
[b] *Department of Radiology and Medical Informatics, University of Geneva, Geneva, Switzerland*
[c] *Developmental Imaging an Psychopathology Laboratory, Office Médico-Pédagogique, Department of Psychiatry, University of Geneva, Geneva, Switzerland*
[d] *Department of Bioengineering, University of Pennsylvania, Philadelphia, PA, United States*
[e] *Department of Electrical & Systems Engineering, University of Pennsylvania, Philadelphia, PA, United States*
[f] *Department of Neurology, University of Pennsylvania, Philadelphia, PA, United States*
[g] *Department of Physics & Astronomy, University of Pennsylvania, Philadelphia, PA, United States*
[h] *Department of Psychiatry, University of Pennsylvania, Philadelphia, PA, United States*

Abstract

How the brain's white-matter anatomy constrains brain activity is an open question that might give insights into the mechanisms that underlie mental disorders such as schizophrenia. Chromosome 22q11.2 deletion syndrome (22q11DS) is a neurodevelopmental disorder with an extremely high risk for psychosis providing a test case to study developmental aspects of schizophrenia. In this study, we used principles from network control theory to probe the implications of aberrant structural connectivity for the brain's functional dynamics in 22q11DS. We retrieved brain states from resting-state functional magnetic resonance images of 78 patients with 22q11DS and 85 healthy controls, and we compared them in terms of persistence control energy based on individual structural connectivity. Control energy was altered in a broad pattern of brain states including both energetically more demanding and less demanding brain states in 22q11DS. Further, we discovered that the brain minimizes energy by spending less time in energetically demanding brain states. In patients with 22q11DS, this behavior was less pronounced, suggesting a dynamic inefficiency of brain function in the disease. In summary, our results provide initial insights into the dynamic implications of altered structural connectivity in 22q11DS, which might improve our understanding of the mechanisms underlying the disease.

Keywords: 22q11.2 deletion syndrome, network control energy, brain state dynamics, resting-state functional MRI, diffusion MRI

*Corresponding author
Email address: daniela.zoller@epfl.ch (Daniela Zöller)

1. Introduction

The brain is a complex dynamic system and brain function during rest and task can be described in terms of the dynamic activation and interaction of different *brain states*: sets of brain regions that are coherently activating and deactivating (Preti et al., 2017; Karahanoğlu et al., 2017). How the brain's underlying structural backbone constrains and facilitates this dynamic behavior is an intensively studied question in the neuroscience community (Bassett and Sporns, 2017; Honey et al., 2009; Becker et al., 2018). The joint consideration of structural and functional properties is particularly promising to provide a better mechanistic explanation of the causes that underlie brain disorders such as schizophrenia (Braun et al., 2018). In recent years, approaches for the investigation of dynamic properties have proven to be particularly useful in probing brain function in health and disease (Preti et al., 2017; Karahanoğlu et al., 2017; Van Den Heuvel and Fornito, 2014). Schizophrenia, in particular, is – as an extension of the well-accepted dysconnectivity hypothesis (Friston et al., 2016) – increasingly perceived as a disorder of broad alterations in large-scale brain state dynamics (Fornito et al., 2012; Du et al., 2016; Braun et al., 2016). A better insight on how alterations in the brain's structure may lead to such aberrant dynamic activation would improve our understanding of this disease to ultimately improve clinical management and patient outcomes (Braun et al., 2018).

Although initial studies of the relationship between brain structure and function used cross-modal correlations (Honey et al., 2009), more recent advances aim to describe how brain structure influences its function at a more mechanistic level (Bassett and Sporns, 2017; Braun et al., 2018). In particular, by using principles from network control theory, it is possible analyze how the brain's structural topology influences its dynamic function (Gu et al., 2015; Betzel et al., 2016; Gu et al., 2017; Kim et al., 2018). In network control theory approaches, the brain is modeled as a graph defined by its structural connectivity, which can transition between different functional states that are given by the activation of each brain region (or network node). Under the assumption that the brain's state is controlled by a single or multiple brain regions, it is then possible to quantify how the underlying structural architecture facilitates or constrains the system's dynamic behavior. Importantly, the temporal properties are given by a (usually linear) dynamic model and are not directly measured. Initially, this framework was used to examine the controllability of the brain from a single region (Gu et al., 2015), measuring how the structural connectivity of a single region would enable it to drive the entire brain into different states that are easier to reach or more difficult to reach. This single-region approach has provided insights into the role that individual regions play in dynamic brain function. In particular, single-region controllability measures give characteristic profiles for different cognitive brain systems

(Gu et al., 2015), change with development (Tang et al., 2017), track individual differences in impulsivity (Cornblath et al., 2018), and are promising to guide target selection for neurostimulation (Muldoon et al., 2016; Khambhati et al., 2019). In patients with bipolar disorder, single-region controllability was found to be altered in subnetworks with aberrant structural connectivity (Jeganathan et al., 2018).

While it is interesting to study transition to the set of easy-to-reach states, and the set of difficult-to-reach states, the inferences are limited in the sense that we cannot say anything about a particular transition that we might observe in the human brain. This limitation motivated recent extensions of the framework to estimate the control energy that is required for specific trajectories between a precisely defined initial state and a precisely defined target state. A simple intuitive example of such a state transition is the transition from activation of the default mode network (DMN) to activation of the fronto-parietal network (FPN) (Betzel et al., 2016; Gu et al., 2017; Kim et al., 2018). Here, we define a set of brain regions that will act as controllers and we estimate the minimum control energy required to steer the brain from an initial state to a target state by formalizing the problem as an optimization problem. Thus far the method has predominantly been used to examine hypothesis-driven state transitions between cognitive brain states defined by an atlas (Gu et al., 2017; Cui et al., 2018). However, recent work extends this approach to investigate data-driven brain states retrieved from functional magnetic resonance imaging (fMRI) (Braun et al., 2019; Cornblath et al., 2018). In this way, temporal properties of functional brain states (measured using fMRI) can be directly compared to the control energy that would be needed to engage in this brain state based on structural connectivity (measured with diffusion weighted MRI (dMRI)).

Further, a disruption in this relationship between functional activity and required control energy could inform our understanding of altered mechanisms that are relevant to the pathophysiology of psychiatric disorders. Here, we tested this hypothesis in individuals with 22q11DS, a neurodevelopmental disorder characterized by a 30-fold increased risk for developing schizophrenia (McDonald-McGinn et al., 2015). Due to the 30-40 % prevalence of schizophrenia by adulthood (Schneider et al., 2014), the disorder is considered a model for the investigation of developmental risk factors before the onset of full-blown schizophrenia (Insel, 2010; Bassett and Chow, 1999). In 22q11DS, the white matter microstructure and connectivity has been extensively studied, mostly in terms of whole-brain or tract-based diffusivity properties (reviewed in Scariati et al., 2016). Affected white-matter bundles mostly include long-range frontal-frontal, frontal-occipital, and fronto-parietal connections (Scariati et al., 2016; Kikinis et al., 2016; Tylee et al., 2017; Olszewski et al., 2017; Roalf et al., 2017). Only a few studies have thus far examined the characteristics of structural whole-brain networks (Ottet et al., 2013; Kikinis et al., 2013; Ottet et al., 2013; Padula et al., 2017; Váša et al., 2016;

Zhan et al., 2018), also mostly reporting fronto-temporal, fronto-parietal (Ottet et al., 2013,?; Zhan et al., 2018), and limbic dysconnectivity (Ottet et al., 2013; Padula et al., 2015). From a topological perspective, Ottet et al. reported longer path lengths and disconnectivity of the brain's hub regions, specifically, in the frontal lobes (Ottet et al., 2013), and Váša et al. uncovered a 'de-centralization' in 22q11DS with a rerouting of shortest network paths to circumvent an affected core that included frontal, parietal, and subcortical regions (Váša et al., 2016).

Only two studies to date have investigated structural and functional properties at the same time (Padula et al., 2015, 2017) and none so far have attempted to examine the dynamic implications of an altered structural network architecture. In this study, we bridge this gap by combining dynamic fMRI analysis with whole-brain tractography and principles from network control theory to investigate how the brain's white matter connectivity may influence its dynamic behavior and how this relationship is affected in patients with 22q11DS. More specifically, we extracted brain states from resting-state fMRI scans using innovation-driven co-activation patterns (iCAPs), a recently proposed approach for dynamic analysis of large-scale brain states marked by its ability to retrieve spatially and temporally overlapping states (Karahanoglu et al., 2015; Farouj et al., 2017; Zöller et al., 2019a). Then, we calculated the control energy that is required – based on the structural connectivity of the same subjects – to engage in these specific brain states (Braun et al., 2019; Cornblath et al., 2018). In this way, we were able to explicitly investigate the relationship between the brain's structural architecture and its functional activation during rest and how this relationship is altered in patients with 22q11DS.

2. Materials and methods

2.1. Participants

FMRI analyses in this study were conducted on the identical dataset as Zöller et al. (2019b), which included 78 patients with 22q11DS and 85 healthy controls (HCs), aged between 8 and 30 years. For structural connectivity analysis, we used dMRI scans acquired from the same subjects. One patient with 22q11DS and 7 HCs had to be excluded from dMRI analyses because no dMRI scan was recorded for them. Table 1 shows demographic information of the remaining 77 patients with 22q11DS and 78 HCs for which both fMRI and dMRI scans were available.

Prodromal positive and negative psychotic symptoms were assessed only in patients with 22q11DS by means of the structured interview for prodromal symptoms (SIPS; Miller et al., 2003).

Table 1: Participant demographics. N/A = not applicable.

	HC	**22q11DS**	**p-value**
Number of subjects (M/F)	78 (32/46)	77 (37/40)	0.379 (χ^2)
Age mean ± SD	16.39 ± 5.52	17.23 ± 5.39	0.342
(range)	(8.1-30.0)	(8.1-29.7)	
Right handed*	80.00%	77.61%	0.564 (χ^2)
IQ**	110.80 ± 13.75	70.32 ± 12.18	<0.001
Number of subjects meeting criteria for psychiatric diagnosis	**N/A**	**42 (55%)**	
Anxiety disorder	N/A	9	
Attention deficit hyperactivity disorder	N/A	8	
Mood disorder	N/A	5	
Schizophrenia or schizoaffective disorder	N/A	3	
More than one psychiatric disorder	N/A	17	
Number of subjects medicated	**0**	9	
Methylphenidate	0	3	
Anitpsychotics	0	1	
Anticonvulsants	0	1	
More than one class of medication	0	3	

* Handedness was measured using the Edinburgh laterality quotient, right handedness was defined by a score of more than 50. ** IQ was measured using the Wechsler Intelligence Scale for Children–III (Wechsler, 1991) for youth and the Wechsler Adult Intelligence Scale–III (Wechsler, 1997) for adults.

2.2. Image acquisition

MRI scans were recorded at the Centre d'Imagerie BioMédicale (CIBM) in Geneva on a Siemens Trio (12-channel head coil) and a Siemens Prisma (20-channel head coil) 3 Tesla scanner. Supplementary Table §1 contains the number of scans that were recorded before and after the update to the Prisma scanner for each image modality, respectively. There was no significant scanner-by-group interaction. Anatomical images were acquired using a T1-weighted sequence with 192 slices (volumetric resolution = $0.86\times0.86\times1.1\,\mathrm{mm}^3$, TR = 2500 ms, TE = 3 ms, flip angle = 8°, acquisition matrix = 256×256, field of view = 23.5 cm). FMRI scans were recorded with an 8 minute resting-state session at a TR of 2.4 s (volumetric resolution = $1.84\times1.84\times3.2\,\mathrm{mm}^3$, 200 frames, 38 axial slices, slice thickness 3.2 mm, TE=30 ms, 85° flip angle, acquisition matrix 94×128, field of view 96×128). Subjects were instructed to fixate on a cross on the screen, let their minds wander, and not fall asleep. DMRI scans were acquired in 30 directions (b = 1000 $\frac{\mathrm{s}}{\mathrm{mm}^3}$, TR = 8300 ms to 8800 ms, TE = 82 ms, flip angle = 90° to 180°, acquisition matrix = 128×128, field of view = 25.6 cm, 64 axial slices, slice thickness = 2 mm).

2.3. fMRI processing

We preprocessed fMRI scans identically as in Zöller et al. (2019b) using in-house code and functions of statistical parametric mapping (SPM12, http://www.fil.ion.ucl.ac.uk/spm/), Data Processing Assistant for Resting-State fMRI (DPARSF; Yan Chaogan, 2010) and Individual Brain Atlases using Statistical Parametric Mapping (IBASPM; Aleman-Gomez et al., 2006). Briefly, preprocessing steps included functional realignment and spatial smoothing with a Gaussian kernel of 6 mm full width half maximum, co-registration of the structural T1-weighted image to the functional mean, segmentation of anatomical scans using the *Segmentation* algorithm in SPM12 (Ashburner and Friston, 2005), creation of a study-specific template using (DARTEL; Ashburner, 2007), exclusion of the first 5 functional frames, and regression of cerebrospinal fluid and white matter BOLD signals. Volumes with a framewise displacement (FD) larger than 0.5 mm were replaced with the spline interpolation of previous and following frames in order to ensure the constant sampling rate required by the iCAPs implementation. After brain state extraction, motion frames were excluded for the computation of temporal characteristics (see below).

Following preprocessing, we extracted iCAPs from resting-state fMRI scans using openly available MATLAB code (`https://c4science.ch/source/iCAPs`; Karahanoglu et al., 2015; Zöller et al., 2019a). Steps included the hemodynamically-informed deconvolution of fMRI timeseries using total activation (Karahanoglu et al., 2011, 2013; Farouj et al., 2017). Then, significant transients are determined with a two-step thresholding procedure following Karahanoglu et al. (2015) and Zöller et al. (2019a) (temporal threshold: 5-95 %; spatial threshold: 5%of gray matter voxels). ICAPs were determined through temporal clustering on concatenated transient frames of all subjects. According to consensus clustering (Monti et al., 2003), the optimum number of clusters was $K = 17$. Finally, a time course was estimated for each iCAP using spatio-temporal transient-informed regression with soft assignment factor $\xi = 1.3$ (Zöller et al., 2019a), and temporal activation duration was computed from thresholded time courses (z-score $> |1|$) as a percent of the total non-motion scanning time. For a more detailed description of the methods, we refer the interested reader to (Zöller et al., 2019b).

2.4. dMRI processing

DMRI scans were processed using functions from the FSL library (Jenkinson et al., 2012) and from the MRtrix3 toolbox (Tournier et al., 2019). After denoising the dMRI scans (*dwidenoise* in MRtrix), eddy current and motion correction was conducted (*eddy* in FLS). Then, the skull was stripped from eddy-corrected dMRI scans (*bet* in FSL) and a white-matter mask, obtained from segmented anatomical images,

was mapped to the resolution of dMRI scans (*flirt* in FSL) and dilated by one voxel (*maskfilter* in MRtrix). Then, we estimated the single-bundle response function for spherical deconvolution based on the Tournier algorithm (Tournier et al., 2013) and computed the fibre orientation distribution function for every voxel with a constrained spherical deconvolution (Tournier et al., 2007). Deterministic fibre tracking (*SD_Stream* in MRtrix) was applied to reconstruct 10×10^6 streamlines longer than 10 mm, which were subsequently filtered using spherical-deconvolution informed filtering of tractograms (SIFT; Smith et al., 2013) to a number of 1×10^6 streamlines for each subject. The Brainnetome atlas (`http://atlas.brainnetome.org`) was warped from MNI- to subject-space and down-sampled to dMRI resolution using SPM12. Finally, a structural connectivity matrix $\mathbf{A} \in \mathbb{R}^{N_{reg}\times N_{reg}}$ was reconstructed for every subject by counting the streamlines connecting each of the $N_{reg} = 234$ regions in the Brainnetome atlas.

2.5. Minimum control energy

In this study, we used linear control theory for brain network analysis, an approach that uses principles from control and dynamical systems theory to investigate the impact that the brain's structural topology may have on its functional dynamics (Kim and Bassett, 2019; Tang and Bassett, 2018; Lynn and Bassett, 2019). Under the assumption of a linear model of dynamics (Kim and Bassett, 2019), and control from all regions of the brain, we estimated the minimum control energy required to remain in specific brain states. For extended reviews on the control of brain network dynamics, we refer the interested reader to (Tang and Bassett, 2018; Lynn and Bassett, 2019). In the following paragraphs, we describe the linear dynamic model used here, and outline the mathematical basis for the computation of the minimum control energy based on this model, as well as the way in which brain states of interest were defined.

Dynamic model. In order to study how the white-matter anatomy of the brain constrains or facilitates state transitions, we modeled the brain as a continuous linear time-invariant dynamic system following Gu et al. (2017) and Betzel et al. (2016)

$$\dot{\mathbf{x}}(t) = \mathbf{A}_s\mathbf{x}(t) + \mathbf{B}\mathbf{u}(t),$$

in which $\mathbf{x}(t) = [x_1(t), ..., x_{N_{\text{reg}}}(t)]^\top \in \mathbb{R}^{N_{\text{reg}}\times 1}$ is the brain's functional state at timepoint t given by the activity level $x_i(t)$ in each region i. The dynamic behavior of the brain is constrained by the stabilized structural white matter connectivity matrix $\mathbf{A}_s$, which is derived from the original structural connectivity matrix $\mathbf{A}$, where each element A_{ij} is the number of streamlines connecting regions i and j. In order to ensure

stability of the dynamic system, all eigenvalues of $\mathbf{A}_s$ have to be below 0. Therefore, we stabilized the system by dividing the original structural connectivity matrix $\mathbf{A}$ by its largest eigenvalue λ_{max} and subtract the identity matrix $\mathbf{I}$: $\mathbf{A}_s = \frac{\mathbf{A}}{\|\lambda_{max}\|+1} - \mathbf{I}$ (Betzel et al., 2016). The diagonal matrix $\mathbf{B} \in \mathbb{R}^{N_{\text{reg}} \times N_{\text{reg}}}$ specifies the set of control nodes. Throughout this study, we assume that all regions of the brain can be controlled and therefore $\mathbf{B} = \mathbf{I}$. Finally, $\mathbf{u}(t) = [u_1(t), ..., u_{N_{\text{reg}}}(t)]^\top \in \mathbb{R}^{N_{\text{reg}} \times 1}$ contains the control input signals $u_i(t)$ at region i and timepoint t.

Notably, the comparison of different graph models shows that there are marked differences in controllability across different types of networks, indicating that characteristics of brain network controllability are unique and potentially relevant for cognitive function (Wu-Yan et al., 2018).

Minimum persistence control energy. In this study, we wished to investigate the structural control energy that is necessary to remain in a certain brain state $\mathbf{x}$ for a duration T. Throughout this study, we compute control energy for a control horizon of $T = 1$ (Betzel et al., 2016). The optimum control input $\mathbf{u}_{min}$ with minimum control energy can be found by solving (Antsaklis and Michel, 2005)

$$\mathbf{u}^* = \min_{\mathbf{u}} E_{min} = \min_{\mathbf{u}} \int_{t=0}^{T} \mathbf{u}(t)^T \mathbf{u}(t) dt.$$

The analytical solution of this minimization problem is given by the minimum energy

$$E_{min} = \left(\mathbf{x}(T) - e^{\mathbf{A}T}\mathbf{x}(0)\right)^\top \mathbf{W}_r^{-1}(T) \left(\mathbf{x}(T) - e^{\mathbf{A}T}\mathbf{x}(0)\right),$$

with the *reachability Gramian*

$$\mathbf{W}_r(T) = \int_{t=0}^{T} e^{\mathbf{A}(T-t)} \mathbf{B}\mathbf{B}^\top e^{\mathbf{A}^\top (T-t)} dt.$$

The optimal control input with this minimum energy can be explicitly computed for each timepoint t:

$$\mathbf{u}^*(t) = \mathbf{B}^\top e^{\mathbf{A}^\top (T-t)} \mathbf{W}_r^{-1}(T) \left(\mathbf{x}(T) - e^{\mathbf{A}T}\mathbf{x}(0)\right).$$

The required control energy at every brain region is given by $E_i = \int_0^T ||u_i^*(t)||^2 dt$ and the total control input can be computed by summing over all regions $E = \sum_{i=1}^{N_{\text{reg}}} E_i$.

Definition of brain states. We wished to investigate the energy that is required to remain in a certain brain state based on the brain's structural connectivity. To compute the minimum control energy as defined above

for every functional brain state, state vectors $\mathbf{x}_k(0) = \mathbf{x}_k(T)$ were obtained by computing in each region the average normalized spatial map of every iCAP k (see subsection *fMRI processing*). In order to minimize noise susceptibility, we thresholded the brain states at a z-score of 1.5; in other words, regions with an average z-score < 1.5 were set to zero.

2.6. Statistical analysis

Statistical group comparison and brain-behavior analysis were conducted with an identical protocol as in Zöller et al. (2019b).

Group comparisons of duration and persistence control energy. Two-sample t-tests were used to compare functional and structural measures between patients with 22q11DS and HCs, and the false discovery rate (FDR) was used to correct for multiple comparisons.

Multivariate relationship between persistence control energy and age. We used partial least squares correlation (PLSC; Krishnan et al., 2011) to retrieve patterns of age-relationship in persistence control energy (PE) of all iCAPs. The steps of PLSC include

1. Computation of concatenated group-wise correlation matrices $\mathbf{R} = \begin{bmatrix} \mathbf{R}_{\mathrm{HC}} \\ \mathbf{R}_{22\mathrm{q}} \end{bmatrix} = \begin{bmatrix} \mathbf{Y}_{\mathrm{HC}}^{\top}\mathbf{X}_{\mathrm{HC}} \\ \mathbf{Y}_{22\mathrm{q}}^{\top}\mathbf{X}_{22\mathrm{q}} \end{bmatrix}$ between age in $\mathbf{Y} \in 1 \times N_{\mathrm{sub}}$ and PE $\mathbf{X} \in K \times N_{\mathrm{sub}}$ of each brain state $k = 1, ..., K$ and subject $s = 1, ..., N_{\mathrm{sub}}$.
2. Singular value decomposition of $\mathbf{R} = \mathbf{USV}^{\top}$ to obtain a number of latent variables (or 'correlation components'). Singular values on the diagonal of $\mathbf{S}$ indicate the explained correlation by each component, age saliences (or 'age weights') in $\mathbf{U}$ and brain saliences (or 'brain weights') in $\mathbf{V}$ indicate how strongly the corresponding group and brain state contributes to the multivariate correlation between age and PE.
3. Permutation testing with 1000 permutations to test for significance of correlation components, where rows of $\mathbf{X}$ were randomly permuted, while leaving $\mathbf{Y}$ unchanged, in order to estimate the null distribution of singular values $\mathbf{S}$ under assumption of no significant correlation between $\mathbf{Y}$ and $\mathbf{X}$.
4. Bootstrapping with 500 bootstrap samples, obtained through sampling with replacement the observations in $\mathbf{Y}$ and $\mathbf{X}$, to evaluate the stability of age- and brain weights in a significant correlation component.

For a more detailed description of PLSC, we refer the interested reader to (Krishnan et al., 2011; Zöller et al., 2017, 2018, 2019a).

Nuisance variable regression. Age and sex were included as nuisance regressors in group comparisons and only sex was used in age-PLSC analyses. Nuisance regressors were standardized within each group to avoid linear dependence with the effects of interest.

2.7. Relationship between brain state function and structure

In order to assess the relationship between resting-state fMRI activation measures and PE, we compute Pearson correlations between the two measures. First, we computed correlations across subjects for each group and each brain state, resulting in $K = 17$ correlation values per group. We then compared these 17 values between HCs and patients with 22q11DS using a paired t-test. Second, we computed correlations across the $K = 17$ brain states for each subject. We then compared the correlation values between HCs and patients with 22q11DS using a two-sample t-test.

3. Results

3.1. Spatial and temporal properties of resting-state functional states.

Using iCAPs, we extracted 17 functional brain states from the resting-state fMRI scans. The optimal number of states was determined using consensus clustering (Monti et al., 2003). Extracted networks include well-known resting-state brain states, such as DMN, FPN, and salience network (SN) states (see supplementary figure S1). Patients with 22q11DS have significantly altered activation duration in 9 brain states, including both brain states with longer activation duration, and brain states with shorter activation duration (see supplemetary figure S2). For a detailed discussion of temporal properties and their relevance for clinical symptoms in 22q11DS, we refer the interested reader to (Zöller et al., 2019b).

3.2. Aberrant persistence control energy of functional brain states in 22q11DS.

We computed minimum PE of the 17 states for all participants based on their individual structural connectivity matrix. Aberrant structural connectivity in patients with 22q11DS leads to altered PE in 8 out of the 17 brain states (see figure 1). PE was higher in patients with 22q11DS in brain states that involve more posterior and dorsal regions – precuneus / ventral DMN (PREC/vDMN), visuospatial network (VSN), primary visual 2 (PrimVIS2) and auditory / sensorimotor (AUD/SM) – as well as in amygdala / hippocampus (AMY/HIP). Reductions of PE on the other hand were present mainly in brain states including more anterior regions – dorsal anterior cingulate cortex /dorsolateral prefrontal cortex (dACC/dlPFC) and anterior DMN (aDMN) – and also in posterior DMN (pDMN).

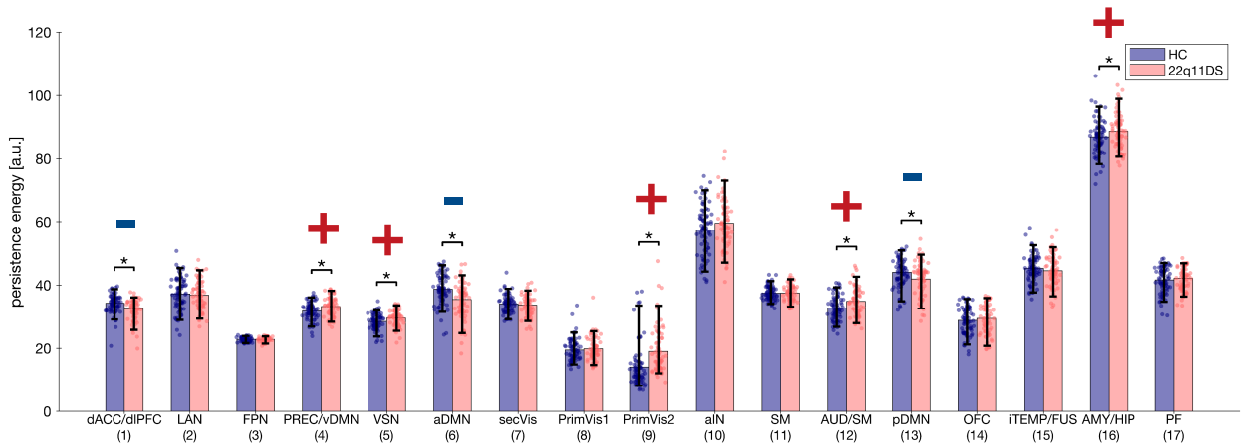

Figure 1: Group differences in PE of the 17 functional brain states in patients with 22q11DS compared to HCs. P-values are FDR-corrected for the 17 multiple comparisons; age and sex were included as covariates. Significant group differences ($p<0.05$) are marked with an asterisk, and with a + (or −) to indicate that they were higher (or lower) in patients. Error bars indicate 5th to 95th percentiles of group distributions. Single-subject duration measures are included as scatterplots. dACC/dlPFC – dorsal anterior cingulate cortex / dorsolateral prefrontal cortex, LAN – language network, FPN – fronto-parietal network, PREC/vDMN – precuneus / ventralDMN, VSN – visuospatial network, aDMN – anterior DMN, SecVIS – secondary visual, PrimVIS1 – primary visual 1, PrimVIS2 – primary visual 2, aIN – anterior insula, SM – sensorimotor, AUD/SM – auditory / sensorimotor, pDMN – posterior DMN, OFC – orbitofrontal cortex, iTEMP/FUS – inferior temporal / fusiform, AMY/HIP – amygdala / hippocampus, PFC – prefrontal cortex.

3.3. Persistence control energy decreases from childhood to adulthood.

There is one significant correlation component ($p<0.001$) resulting from PLSC analysis testing for a relationship between PE and age (see figure 2). PE is negatively correlated with age in 7 out of the 17 states. This correlation with age is significant for both groups, but stronger in patients with 22q11DS than in HCs. Age-related states include anterior and posterior DMN, anterior insula (aIN), sensory states (primary visual 1 (PrimVIS1) and sensorimotor (SM)), one emotional state (AMY/HIP), and the language state. The PE of states that are commonly associated with goal-directed behavior during tasks do not show any relationship with age (i.e., PREC/vDMN, which is sometimes called dorsal attention state, FPN, and VSN)

3.4. No correlation across subjects between activation duration and persistence control energy.

In order to test whether there was a relationship between the measures across subjects, we first considered between group differences. If there was a global linear relationship between structural PE and activation duration across subjects, all states would be altered in both, and always in the same or opposing direction. When comparing alterations of temporal activation and structural PE (see supplementary figure S3), there is, however, no clear pattern of common alterations. While brain states with reduced PE (dACC/dlPFC,

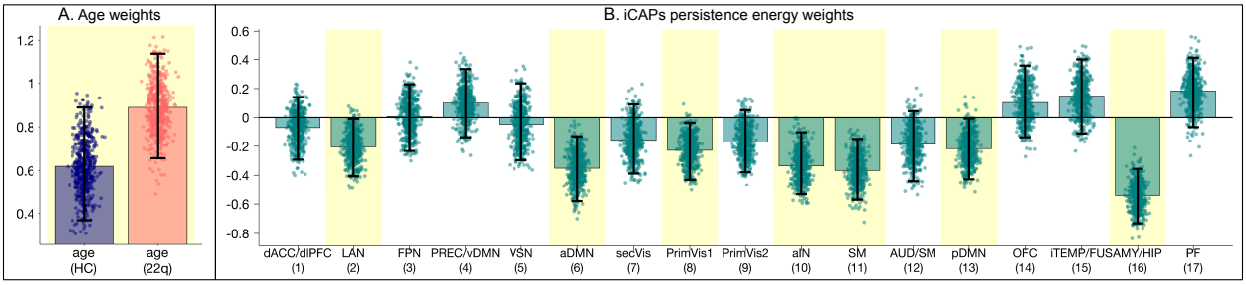

Figure 2: PLSC testing for a relationship between PE and age resulted in one significant correlation component ($p<0.001$). A) According to age weights indicating the correlation strength in each group, the age-relationship is stronger in patients with 22q11DS than in HCs. B) PE weights show that there is a significant negative relationship with age in 7 out of the 17 brain states. Error bars indicate bootstrapping 95% confidence intervals; robust results were indicated by yellow background.

aDMN, and pDMN) have all also reduced activation duration, only AMY/HIP has both increased PE and activation duration, and PrimVIS2 is even altered in different directions. Further, there are multiple brain states that are only affected in one single modality. FPN, SM, orbitofrontal cortex (OFC), inferiortemporal / fusiform (iTEMP/FUS) have only aberrant activation duration, while PREC/vDMN, VSN and AUD/SM are only affected in terms of PE.

To explicitly test for a linear relationship between resting-state activation duration and structural PE in every state separately, we computed correlations between the two measures across subjects for each state. As already expected based on the observations on group differences in both modalities, there was no significant correlation between the two measures either in patients with 22q11DS or in HCs (see figure 3A). In other words, a subject who spends a long time in one brain state, does not have a systematically higher or lower PE of that brain state compared to other subjects.

3.5. Negative correlation across states between activation duration and persistence control energy.

To test whether within each subject there was a relationship between temporal activation and structural PE, we computed across-states correlations for each subject (see figure 3B). There was indeed a negative correlation between activation duration and PE. In other words, all subjects tend to spend less time in brain states whose structural wiring leads to higher PE. This negative correlation was significantly stronger (lower) in HCs than in patients with 22q11DS ($p=0.010$).

Finally, we tested for a relationship with age of these negative correlation values (see figure 4). In HCs the energy-activation correlation did not change over age ($c=-0.03$, $p=0.937$). In patients with 22q11DS, however, the correlation became significantly weaker (higher negative values) with increasing age ($c=0.37$, $p=0.005$). In a joint model, the group-by-age interaction was significant with $p=0.002$. In other words,

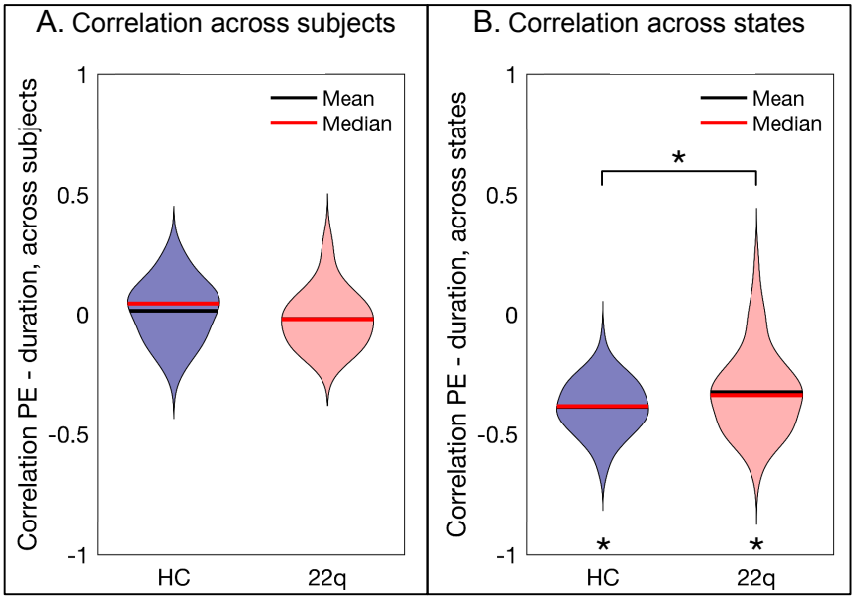

Figure 3: Correlation between structural PE and resting-state activation duration. A) Across subjects there is no significant correlation, either in patients with 22q11DS or in HCs. Violin plots show the distribution of correlations for all brain states. B) Across states there is a negative correlation between the two modalities: the higher the PE, the shorter the resting-state activation duration. This correlation is significantly stronger in HCs than in patients with 22q11DS. Violin plots show the distribution of correlations for all subjects. Significant group differences ($p<0.05$) are marked with an asterisk.

while at a younger age, patients showed similar energy-activation relationship as HCs, older patients have a weaker negative energy-activation correlation, indicating that the observed weakening in correlation (see previous paragraph) is emerging over age.

There was no correlation with full-scale intelligence quotient (FSIQ; HCs: c=0.08,p=0.728; 22q11DS: c=-0.01, p=0.0.937), positive psychotic symptoms as measured by the sum of positive SIPS scores (22q11DS: c=-0.12, p=0.688) and negative psychotic symptoms as measured by the sum of negative SIPS scores (22q11DS: c=-0.37, p=0.130). Reported p-values were corrected for the six computed correlations using the FDR.

4. Discussion

Here we used dynamic models to investigate the relationship between structural brain connectivity and its functional activation in 22q11DS, a population at extremely high risk for schizophrenia. Combining fMRI activation analysis with network control energy, we probed the possible mechanistic implications of aberrant brain structure on altered functional activation (Braun et al., 2018). Functional brain states were retrieved from dynamic changes of resting-state functional activity. Then, we used network control theory to analyze how the white matter anatomy of these brain states may influence their dynamic behavior (Braun et al., 2019; Cornblath et al., 2018). We found aberrant control energy of several brain states, mainly

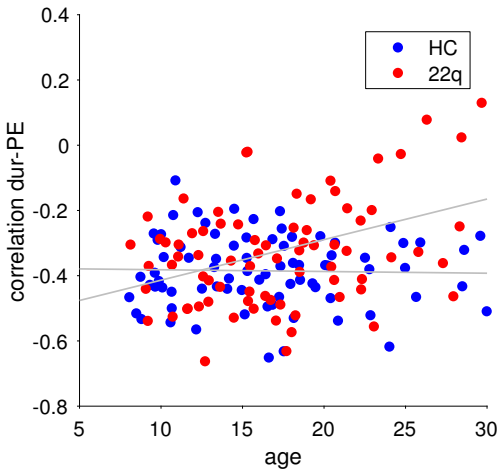

Figure 4: The negative correlation between PE and activation duration is constant over age in HCs (c=-0.03, p=0.937), but significantly increasing (i.e., weakening) with higher age in patients with 22q11DS (c=0.38, p=0.005).

involving anterior or posterior medial connections. Further, PE decreased from childhood to adulthood both in patients with 22q11DS and HCs. Finally, when probing for a relationship between structural control energy and functional resting-state activation, we found a negative correlation across brain states consistent with prior work (Cornblath et al., 2018), and which was less pronounced in patients with 22q11DS. However, we found no direct relationship between control energy of a brain state and its functional activation across subjects. In the following exposition, we will first discuss the alterations of PE and structure-function inefficiency in patients with 22q11DS, and then offer a tentative explanation for the absence of an across-subject relationship between control energy and functional activation.

4.1. Anterior-posterior and medial-lateral gradient of altered connectivity leads to aberrant brain control energy in 22q11DS

We analyzed persistence control energy of resting-state brain states in 22q11DS and found that aberrant structural wiring leads to a pattern of altered controllability with some brain states requiring higher energy and others requiring lower control energy. Persistence energy is mainly reduced in frontal brain states (aDMN, dACC/dlPFC) and increased in occipital (PREC/vDMN, PrimVIS2) and lateral parietal (VSN, AUD/SM) brain states. This pattern of findings confirms prior reports of aberrant anterior-posterior and medial-lateral white-matter connectivity in patients with 22q11DS (Scariati et al., 2016; Gothelf et al., 2011; Váša et al., 2016). Our study expands upon these prior studies by probing the impact of this aberrant wiring on the dynamic behavior of the brain in terms of the energy that is needed to engage in these brain states.

In particular, we found reduced persistence control energy in DMN and cingulo-frontal SN, which are

two brain systems that are known to play a central role in higher order cognition (Menon, 2011). Previous reports provide evidence that their structural and functional connectivity is altered in patients with 22q11DS (Padula et al., 2015, 2017; Schreiner et al., 2014). In particular the dACC, which is a central node of the SN, has been found to be affected in 22q11DS using different neuroimaging modalities and has been suggested as a biomarker for psychosis in the disorder (Padula et al., 2018). Of note, these states were also found to have altered resting-state activation (Zöller et al., 2019b) and even though we here did not find a linear relationship between resting-state activation duration and structural control energy, the fact that a majority of brain states is affected in both measures suggests that there may be a more complex underlying common mechanism.

Moreover, we found that persistence in the amygdala and hippocampus brain state was energetically more demanding for patients with 22q11DS, but nevertheless those same patients spent more of the resting-state scan time engaging in this state. The amygdala plays a central role in emotion processing and anxiety (Etkin and Wager, 2007), which is an important behavioral risk factor for psychosis in 22q11DS (Gothelf et al., 2007, 2013). In line with this literature on the role of the amygdala, we recently found that higher functional activation and aberrant coupling of this amygdala and hippocampus brain state tracks with higher levels of anxiety (Zöller et al., 2019b). Further, in a recent study we found that a developmental decrease in hippocampal volume during adolescence is related to the emergence of psychotic symptoms (Mancini et al., 2019). The results presented here confirm that amygdala and hippocampus are also affected in terms of structural connectivity, which in turn leads to aberrant controllability properties in patients with 22q11DS. Future studies should examine whether this aberrant wiring is related to altered developmental trajectories, and whether it is linked to higher levels of anxiety and the risk for developing psychosis.

4.2. The brain gets energetically more efficient from childhood to adulthood

Aside from alterations in 22q11DS, we found that persistence control energy of many brain states (7 out of 17) is negatively correlated with age, both in patients with 22q11DS and in HCs. This finding suggests that with increasing age, the brain gets more efficiently wired to reduce the control energy required for its functional activation. In line with these findings, Tang et al. found that both average and modal controllability (which measure the general ability to steer the brain towards easy-to-reach or difficult-to-reach brain states) increase over age in a similar age range, which suggests an increasingly efficient wiring that at the same time allows a higher diversity of brain dynamics (Tang et al., 2017). Importantly, while there are small variations in the distributions of controllability across the brain in males and females, the trend for increasing controllability with age is equally strong in both sexes (Cornblath et al., 2018). Further, Cui et al.

(2018) found that control energy of atlas-based brain states calculated with a comparable approach to ours, was also decreasing from childhood to adulthood in most brain states (Cui et al., 2018). This developmental trajectory of structural brain architecture was preserved in patients, suggesting that while they present with absolute alterations of controllability properties, their overall development seems to be largely intact.

4.3. Dynamic inefficiency in patients with 22q11DS, which becomes increasingly marked with age

Finally, when investigating the relationship between functional activation and structural control energy, we found that the brain activates in a highly efficient way, spending less time in brain states that are energetically more demanding, consistent with prior evidence in a completely different cohort (Cornblath et al., 2018). In patients with 22q11DS, this relationship was significantly weaker than in HCs, which suggests that aside from the pure alteration in structure and function, the relationship between the two is also altered. In particular, patients use their brains in a less efficient way, spending more time in energetically demanding states than HCs. Additionally, this dynamic inefficiency in patients with 22q11DS became increasingly marked with greater age. Possibly, the patients' inefficient use of their brain may express in the more severe symptomatology characteristic of older patients. Divergent trajectories during adolescence have for instance been reported for executive functions (Maeder et al., 2016). However, here we did not find a significant correlation between our measure of dynamic efficiency and psychotic symptoms or IQ, possibly because of our limited sample size. Therefore, our hypothesis should be verified in future studies with larger sample sizes, and targeting more specific measures of particular clinical symptoms and executive functions.

4.4. Control energy and activation of a single state are not correlated across subjects

While we were able to detect a relationship between functional activation and structural control energy across states (pointing towards the inherent efficiency of the human brain as discussed above), we did not observe a relationship across subjects. In other words, subjects with less efficiently wired brain states (higher PE) did not spend more or less time in these brain states compared to other subjects. A possible explanation may be that, while here we were testing for a simple relationship for each state separately, the association is likely more complex than a one-to-one linear correlation. Importantly, brain states to not act in isolation, but interact among themselves. For instance, knowing about the interaction between the DMN and the amygdala and hippocampus that we discovered in the same dataset (Zöller et al., 2019b), one could imagine that indeed alterations of controllability in the DMN may lead to increased activity of the amygdala and hippocampus. Testing for such cross-network relationships may be even more interesting, and our methological approach offers a valuable framework to explore this complexity in future research.

4.5. Methodological considerations and limitations

Placement among existing state-of-the-art control strategies. The approaches using control theory to analyze brain networks can be differentiated based on the control strategies they use. Initial studies on controllability of brain networks examined properties like average and modal controllability, which assess the ease of a local or distant state transition while ignoring the nature of either the initial or target states (e.g., Gu et al., 2015; Tang et al., 2017; Jeganathan et al., 2018). Studies on specific state trajectories, on the other hand, stipulate the initial and target states and assess the energy necessary for that specific trajectory (Gu et al., 2017; Betzel et al., 2016; Cui et al., 2018). In this case, states could be defined either by activating all regions in a cognitive system defined from the literature (Gu et al., 2017; Betzel et al., 2016; Cui et al., 2018), or by choosing a data-derived brain state (Cornblath et al., 2018; Braun et al., 2019). Similar to the latter two studies (Cornblath et al., 2018; Braun et al., 2019), here we investigated transitions between specific states, and we defined the brain states in a data-driven way from fMRI data acquired from the same subjects. Using this approach, we found profound differences in control energy of multiple states in patients with 22q11DS. These findings underline the potential of data-driven brain states to detect relevant subject-specific alterations, which is promising for future studies involving other clinical populations.

Variance of structural connectivity across subjects and across regions has different scales. In the present study, structural connectivity was measured in terms of connection density; that is, with a fixed number of reconstructed streamlines. As a result, the variability of connectivity across regions is relatively high compared to the variability across subjects. Therefore, this approach supports a careful investigation into *relative* changes in connectivity, but it is less powerful in tracking *absolute* changes in connectivity. In our results, this effect can be observed in figure 1, where the differences in energy from one state to another are much larger than the differences in persistence energy across subjects for one single brain state. Significant differences between subjects do exist, however, they are small with respect to the differences between brain states. This effect may be a possible reason why we detected correlations with functional activation across brain states, but not across subjects.

Linear models of brain dynamics. For simplicity, here we chose to use a linear model of dynamics on the structural connectivity graph (Kim and Bassett, 2019; Honey et al., 2009; Gu et al., 2015) to calculate minimum control energy (Betzel et al., 2016). Even though this model is the most widely used approach for network control theory in neuroscience, it may be overly simplistic. Incorporating models of non-linear dynamics could prove useful in the future as they could potentially improve the estimation of more realistic

control energy (Kim and Bassett, 2019). It is possible that an estimate based on more biologically plausible dynamic models would allow us to detect more subtle relationships between controllability and functional activation.

5. Conclusion

In this study, we investigated the control energy of functional brain states in patients with 22q11DS. This is the first study investigating the impact of aberrant structural connectivity on brain dynamics using control energy in 22q11DS. We found that altered connectivity in patients with 22q11DS leads to reduced energy impact for engaging frontal brain states, whereas more occipital and parietal brain states were energetically more demanding for patients with 22q11DS than HCs. Further, in a comparison of structural control energy with resting-state fMRI activation, we found that the brain functions in an efficient way by engaging less in energetically demanding brain states. In patients with 22q11DS the anticorrelation between activation and control energy is weaker than in controls, suggesting a dynamic inefficiency of brain function in these patients. In summary, we contribute one of the first studies investigating a direct link between control energy and functional activation during rest and provide promising insights for a better understanding of brain alterations in 22q11DS.

Acknowledgements

We are grateful to the subjects who participated in our study and thank Sarah Menghetti, Léa Chambaz, Virginie Pouillard and Dr. Maude Schneider for their involvement with the participants. We would also like to acknowledge Prof. François Lazeyras and the CIBM group for their support during data collection.

This work was supported by the Swiss National Science Foundation (SNSF) under Grants 32473B_121966, 234730_144260 and 145250 to SE, and Grant 163859 to MS, and by the National Center of Competence in Research (NCCR) "SYNAPSY - The Synaptic Bases of Mental Diseases", SNSF, under Grants 51AU40_125759, 51NF40_158776 and 51NF40-185897.

DSB acknowledges support from the John D. and Catherine T. MacArthur Foundation, the Alfred P. Sloan Foundation, the ISI Foundation, the Paul Allen Foundation, the Army Research Laboratory (W911NF-10-2-0022), the Army Research Office (Bassett-W911NF-14-1-0679, DCIST- W911NF-17-2-0181, W911NF-16-1-0474), the National Institute of Mental Health (2-R01-DC-009209-11, R01-MH112847, R01-MH107235, R21-M MH-106799), the National Institute of Child Health and Human Development (1R01HD086888-01), the National Institute of Neurological Disorders and Stroke (R01 NS099348), and the National Science

Foundation (BCS-1441502, BCS-1430087, NSF PHY-1554488 and BCS-1631550). The content is solely the responsibility of the authors and does not necessarily represent the official views of any of the funding agencies.

Data availability statement

The data that support the findings of this study are available on request from the corresponding author. The data are not publicly available due to privacy or ethical restrictions.

Conflict of interest

The authors have no conflict of interest to declare.

References

Aleman-Gomez, Y., Melie-García, L., and Valdés-Hernandez, P. (2006). IBASPM: toolbox for automatic parcellation of brain structures. In *12th Annu. Meet. Organ. Hum. Brain Mapp.*

Antsaklis, P. J. and Michel, A. N. (2005). *Linear Systems*. Birkhäuser Boston.

Ashburner, J. (2007). A fast diffeomorphic image registration algorithm. *Neuroimage*, 38(1):95–113. doi: 10.1016/j.neuroimage.2007.07.007.

Ashburner, J. and Friston, K. J. (2005). Unified segmentation. *Neuroimage*, 26(3):839–851. doi: 10.1016/j.neuroimage.2005.02.018.

Bassett, A. S. and Chow, E. W. C. (1999). 22q11 deletion syndrome: A genetic subtype of schizophrenia. *Biol. Psychiatry*, 46(7):882–891. doi: 10.1016/S0006-3223(99)00114-6.

Bassett, D. S. and Sporns, O. (2017). Network neuroscience. *Nat. Neurosci.*, 20(3):353. doi: 10.1038/nn.4502.

Becker, C. O., Pequito, S., Pappas, G. J., Miller, M. B., Grafton, S. T., Bassett, D. S., and Preciado, V. M. (2018). Spectral mapping of brain functional connectivity from diffusion imaging. *Sci. Rep.*, 8(1):1–15. doi: 10.1038/s41598-017-18769-x.

Betzel, R. F., Gu, S., Medaglia, J. D., Pasqualetti, F., and Bassett, D. S. (2016). Optimally controlling the human connectome: The role of network topology. *Sci. Rep.*, 6:1–14. doi: 10.1038/srep30770.

Braun, U., Schäfer, A., Bassett, D. S., Rausch, F., Schweiger, J. I., Bilek, E., Erk, S., Romanczuk-Seiferth, N., Grimm, O., Geiger, L. S., Haddad, L., Otto, K., Mohnke, S., Heinz, A., Zink, M., Walter, H., Schwarz, E., Meyer-Lindenberg, A., and Tost, H. (2016). Dynamic brain network reconfiguration as a potential schizophrenia genetic risk mechanism modulated by NMDA receptor function. *Proc. Natl. Acad. Sci.*, 113(44):12568–12573. doi: 10.1073/pnas.1608819113.

Braun, U., Schaefer, A., Betzel, R. F., Tost, H., Meyer-Lindenberg, A., and Bassett, D. S. (2018). From Maps to Multi-dimensional Network Mechanisms of Mental Disorders. *Neuron*, 97(1):14–31. doi: 10.1016/j.neuron.2017.11.007.

Braun, U., Harneit, A., Pergola, G., Merana, T., Schaefer, A., Betzel, R., Zang, Z., Schweiger, J. I., Schwartz, K., Chen, J., Blasi, G., Bertolino, A., Durstewitz, D., Pasqualetti, F., Schwarz, E., Meyer-Lindenberg, A., Bassett, D. S., and Tost, H. (2019). Brain state stability during working memory is explained by network control theory, modulated by dopamine D1/D2 receptor function, and diminished in schizophrenia. *bioRxiv Prepr.*, 679670. doi: 10.1101/679670.

Cornblath, E. J., Ashourvan, A., Kim, J. Z., Betzel, R. F., Ciric, R., Baum, G. L., He, X., Ruparel, K., Moore, T. M., Gur, R. C., Gur, R. E., Shinohara, R. T., Roalf, D. R., Satterthwaite, T. D., and Bassett, D. S. (2018). Context-dependent architecture of brain state dynamics is explained by white matter connectivity and theories of network control. *bioRxiv Prepr.*, 412429. doi: 10.1101/412429.

Cornblath, E. J., Tang, E., Baum, G. L., Moore, T. M., Adebimpe, A., Roalf, D. R., Gur, R. C., Gur, R. E., Pasqualetti, F., Satterthwaite, T. D., and Bassett, D. S. (2018). Sex differences in network controllability as a predictor of executive function in youth. *Neuroimage*, 188:122–134. doi: 10.1016/j.neuroimage.2018.11.048.

Cui, Z., Stiso, J., Baum, G. L., Kim, J. Z., Roalf, D. R., Betzel, R. F., Gu, S., Lu, Z., Xia, C. H., Ciric, R., Moore, T. M., Shinohara, R. T., Ruparel, K., Davatzikos, C., Pasqualetti, F., Gur, R. E., Gur, R. C., Bassett, D. S., and Satterthwaite, T. D. (2018). Optimization of Energy State Transition Trajectory Supports the Development of Executive Function During Youth. *bioRxiv Prepr.*, 424929. doi: 10.1101/424929.

Du, Y., Pearlson, G. D., Yu, Q., He, H., Lin, D., Sui, J., Wu, L., and Calhoun, V. D. (2016). Interaction among subsystems within default mode network diminished in schizophrenia patients: A dynamic connectivity approach. *Schizophr. Res.*, 170(1):55–65. doi: 10.1016/j.schres.2015.11.021.

Etkin, A. and Wager, T. (2007). Reviews and Overviews Functional Neuroimaging of Anxiety : A Meta-Analysis of Emotional Processing in PTSD , Social Anxiety Disorder , and Specific Phobia. *Am. J. Psychiatry*, 164(October):1476–1488. doi: 10.1078/1439-1791-00175.

Farouj, Y., Karahanoglu, F. I., and Van De Ville, D. (2017). Regularized Spatiotemporal Deconvolution of fMRI Data Using Gray-Matter Constrained Total Variation. *Proc. 14th IEEE Int. Symp. Biomed. Imaging From Nano to Macro*, pages 472–475.

Fornito, A., Zalesky, A., Pantelis, C., and Bullmore, E. T. (2012). Schizophrenia, neuroimaging and connectomics. *Neuroimage*, 62(4):2296–2314. doi: 10.1016/j.neuroimage.2011.12.090.

Friston, K., Brown, H. R., Siemerkus, J., and Stephan, K. E. (2016). The dysconnection hypothesis (2016). *Schizophr. Res.*, 176(2-3):83–94. doi: 10.1016/j.schres.2016.07.014.

Gothelf, D., Feinstein, C., Thompson, T., Gu, E., Penniman, L., Van Stone, E., Kwon, H., Eliez, S., and Reiss, A. L. (2007). Risk factors for the emergence of psychotic disorders in adolescents with 22q11.2 deletion syndrome. *Am. J. Psychiatry*, 164(4):663–669. doi: 10.1176/ajp.2007.164.4.663.

Gothelf, D., Hoeft, F., Ueno, T., Sugiura, L., Lee, A. D., Thompson, P., and Reiss, A. L. (2011). Developmental changes in multivariate neuroanatomical patterns that predict risk for psychosis in 22q11.2 deletion syndrome. *J. Psychiatr. Res.*, 45(3):322–331. doi: 10.1016/j.jpsychires.2010.07.008.

Gothelf, D., Schneider, M., Green, T., Debbané, M., Frisch, A., Glaser, B., Zilkha, H., Schaer, M., Weizman, A., and Eliez, S. (2013). Risk factors and the evolution of psychosis in 22q11.2 deletion syndrome: A longitudinal 2-site study. *J. Am. Acad. Child Adolesc. Psychiatry*, 52(11). doi: 10.1016/j.jaac.2013.08.008.

Gu, S., Pasqualetti, F., Cieslak, M., Telesford, Q. K., Yu, A. B., Kahn, A. E., Medaglia, J. D., Vettel, J. M., Miller, M. B., Grafton, S. T., and Bassett, D. S. (2015). Controllability of structural brain networks. *Nat. Commun.*, 6:8414. doi: 10.1038/ncomms9414.

Gu, S., Betzel, R. F., Mattar, M. G., Cieslak, M., Delio, P. R., Grafton, S. T., Pasqualetti, F., and Bassett, D. S. (2017). Optimal trajectories of brain state transitions. *Neuroimage*, 148(January):305–317. doi: 10.1016/j.neuroimage.2017.01.003.

Honey, C. J., Sporns, O., Cammoun, L., Gigandet, X., Thiran, J.-P., Meuli, R., and Hagmann, P. (2009). Predicting human

resting-state functional connectivity. *Proc. Natl. Acad. Sci.*, 106(6):2035–2040. doi: 10.1073/pnas.0811168106.

Insel, T. R. (2010). Rethinking schizophrenia. *Nature*, 468(7321):187–193. doi: 10.1038/nature09552.

Jeganathan, J., Perry, A., Bassett, D. S., Roberts, G., Mitchell, P. B., and Breakspear, M. (2018). Fronto-limbic dysconnectivity leads to impaired brain network controllability in young people with bipolar disorder and those at high genetic risk. *NeuroImage Clin.*, 19(March):71–81. doi: 10.1016/j.nicl.2018.03.032.

Jenkinson, M., Beckmann, C. F., Behrens, T. E., Woolrich, M. W., and Smith, S. M. (2012). Fsl. *Neuroimage*, 62(2):782–790. doi: 10.1016/j.neuroimage.2011.09.015.

Karahanoglu, F. I., Bayram, I., and Van De Ville, D. (2011). A Signal Processing Approach to Generalized 1-D Total Variation. *IEEE Trans. Signal Process.*, 59(11):5265–5274.

Karahanoglu, F. I., Caballero-Gaudes, C., Lazeyras, F., and Van De Ville, D. (2013). Total activation: FMRI deconvolution through spatio-temporal regularization. *Neuroimage*, 73:121–134. doi: 10.1016/j.neuroimage.2013.01.067.

Karahanoglu, F. I., Van De Ville, D., Karahanoğlu, F. I., and Van De Ville, D. (2015). Transient brain activity disentangles fMRI resting-state dynamics in terms of spatially and temporally overlapping networks. *Nat. Commun.*, 6:7751. doi: 10.1038/ncomms8751.

Karahanoğlu, F. I., Van De Ville, D., Karahanoglu, F. I., and Van De Ville, D. (2017). Dynamics of large-scale fMRI networks: Deconstruct brain activity to build better models of brain function. *Curr. Opin. Biomed. Eng.*, 3:28–36. doi: 10.1016/j.cobme.2017.09.008.

Khambhati, A. N., Kahn, A. E., Costantini, J., Ezzyat, Y., Solomon, E. A., Gross, R. E., Jobst, B. C., Sheth, S. A., Zaghloul, K. A., Worrell, G., Seger, S., Lega, B. C., Weiss, S., Sperling, M. R., Gorniak, R., Das, S. R., Stein, J. M., Rizzuto, D. S., Kahana, M. J., Lucas, T. H., Davis, K. A., Tracy, J. I., and Bassett, D. S. (2019). Functional control of electrophysiological network architecture using direct neurostimulation in humans. *Netw. Neurosci.*, 0(0:0):1–30. doi: 10.1101/292748.

Kikinis, Z., Makris, N., Finn, C. T., Bouix, S., Lucia, D., Coleman, M. J., Tworog-Dube, E., Kikinis, R., Kucherlapati, R., Shenton, M. E., and Kubicki, M. (2013). Genetic contributions to changes of fiber tracts of ventral visual stream in 22q11.2 deletion syndrome. *Brain Imaging Behav.*, 7(3):316–325. doi: 10.1007/s11682-013-9232-5.

Kikinis, Z., Cho, K. I. K., Coman, I. L., Radoeva, P. D., Bouix, S., Tang, Y., Eckbo, R., Makris, N., Kwon, J. S., Kubicki, M., Antshel, K. M., Fremont, W., Shenton, M. E., and Kates, W. R. (2016). Abnormalities in brain white matter in adolescents with 22q11.2 deletion syndrome and psychotic symptoms. *Brain Imaging Behav.*, 11(5):1353–1364. doi: 10.1007/s11682-016-9602-x.

Kim, J. Z. and Bassett, D. S. (2019). Linear Dynamics & Control of Brain Networks. *arXiv Prepr.*, 1902.03309.

Kim, J. Z., Soffer, J. M., Kahn, A. E., Vettel, J. M., Pasqualetti, F., and Bassett, D. S. (2018). Role of graph architecture in controlling dynamical networks with applications to neural systems. *Nat. Phys.*, 14(1):91–98. doi: 10.1038/nphys4268.

Krishnan, A., Williams, L. J., McIntosh, A. R., and Abdi, H. (2011). Partial Least Squares (PLS) methods for neuroimaging: A tutorial and review. *Neuroimage*, 56(2):455–475. doi: 10.1016/j.neuroimage.2010.07.034.

Lynn, C. W. and Bassett, D. S. (2019). The physics of brain network structure, function and control. *Nat. Rev. Phys.*, 1(5):318–332. doi: 10.1038/s42254-019-0040-8.

Maeder, J., Schneider, M., Bostelmann, M., Debbané, M., Glaser, B., Menghetti, S., Schaer, M., and Eliez, S. (2016). Developmental trajectories of executive functions in 22q11.2 deletion syndrome. *J. Neurodev. Disord.*, 8(1):10. doi: 10.1186/s11689-016-9141-1.

Mancini, V., Sandini, C., Padula, M. C., Zöller, D., Schneider, M., Schaer, M., and Eliez, S. (2019). Positive psychotic symptoms

are associated with divergent developmental trajectories of hippocampal volume during late adolescence in patients with 22q11DS. *Mol. Psychiatry*, d. doi: 10.1038/s41380-019-0443-z.

McDonald-McGinn, D. M., Sullivan, K. E., Marino, B., Philip, N., Swillen, A., Vorstman, J. A. S., Zackai, E. H., Emanuel, B. S., Vermeesch, J. R., Morrow, B. E., Scambler, P. J., and Bassett, A. S. (2015). 22q11.2 deletion syndrome. *Nat. Rev. Dis. Prim.*, 1(November):15071. doi: 10.1016/B978-0-323-44548-1.00154-6.

Menon, V. (2011). Large-scale brain networks and psychopathology: A unifying triple network model. *Trends Cogn. Sci.*, 15(10):483–506. doi: 10.1016/j.tics.2011.08.003.

Miller, T. J., Mcqlashan, T. H., Rosen, J. L., Cadenhead, K., Ventura, J., Mcfarlane, W., Perkins, D. O., Pearlson, Q. D., and Woods, S. W. (2003). Prodromal Assessment With the Structured Interview for Prodromal Syndromes and the Scale of Prodromal Symptoms: Predictive Validity, Interrater Reliability, and Training to Reliability. *Schizophr. Bull.*, 29(4):703–715. doi: 10.1093/oxfordjournals.schbul.a007040.

Monti, S., Tamayo, P., Mesirov, J., and Golub, T. (2003). Consensus Clustering: A Resampling-Based Method for Class Discovery and Visualization of Gene Expression Microarray Data. *Mach. Learn.*, 52(1):91–118. doi: 10.1023/A:1023949509487.

Muldoon, S. F., Pasqualetti, F., Gu, S., Cieslak, M., Grafton, S. T., Vettel, J. M., and Bassett, D. S. (2016). Stimulation-based control of dynamic brain networks. *PLoS Comput. Biol.*, 12(9):e1005076. doi: 10.1371/journal.pcbi.1005076.

Olszewski, A. K., Kikinis, Z., Gonzalez, C. S., Coman, I. L., Makris, N., Gong, X., Rathi, Y., Zhu, A., Antshel, K. M., Fremont, W., Kubicki, M. R., Bouix, S., Shenton, M. E., and Kates, W. R. (2017). The social brain network in 22q11.2 deletion syndrome: A diffusion tensor imaging study. *Behav. Brain Funct.*, 13(1):1–17. doi: 10.1186/s12993-017-0122-7.

Ottet, M.-C., Schaer, M., Cammoun, L., Schneider, M., Debbané, M., Thiran, J.-P., and Eliez, S. (2013). Reduced fronto-temporal and limbic connectivity in the 22q11.2 deletion syndrome: vulnerability markers for developing schizophrenia? *PLoS One*, 8(3):e58429. doi: 10.1371/journal.pone.0058429.

Ottet, M.-C., Schaer, M., Debbané, M., Cammoun, L., Thiran, J.-P., and Eliez, S. (2013). Graph theory reveals dysconnected hubs in 22q11DS and altered nodal efficiency in patients with hallucinations. *Front. Hum. Neurosci.*, 7(September). doi: 10.3389/fnhum.2013.00402.

Padula, M. C., Schaer, M., Scariati, E., Schneider, M., Van De Ville, D., Debbané, M., and Eliez, S. (2015). Structural and functional connectivity in the default mode network in 22q11.2 deletion syndrome. *J Neurodev Disord*, 7(1):23. doi: 10.1186/s11689-015-9120-y.

Padula, M. C., Scariati, E., Schaer, M., Sandini, C., Ottet, M. C., Schneider, M., Van De Ville, D., and Eliez, S. (2017). Altered structural network architecture is predictive of the presence of psychotic symptoms in patients with 22q11.2 deletion syndrome. *NeuroImage Clin.*, 16(July):142–150. doi: 10.1016/j.nicl.2017.07.023.

Padula, M. C., Schaer, M., Scariati, E., Maeder, J., Schneider, M., and Eliez, S. (2017). Multimodal investigation of triple network connectivity in patients with 22q11DS and association with executive functions. *Hum. Brain Mapp.*, 2189(January):2177–2189. doi: 10.1002/hbm.23512.

Padula, M. C., Scariati, E., Schaer, M., and Eliez, S. (2018). A Mini Review on the Contribution of the Anterior Cingulate Cortex in the Risk of Psychosis in 22q11.2 Deletion Syndrome. *Front. Psychiatry*, 9(August):9–14. doi: 10.3389/fpsyt.2018.00372.

Preti, M. G., Bolton, T. A. W., and Van De Ville, D. (2017). The dynamic functional connectome: State-of-the-art and perspectives. *Neuroimage*, 160(December):41–54. doi: 10.1016/j.neuroimage.2016.12.061.

Roalf, D. R., Eric Schmitt, J., Vandekar, S. N., Satterthwaite, T. D., Shinohara, R. T., Ruparel, K., Elliott, M. A., Prab-

hakaran, K., McDonald-McGinn, D. M., Zackai, E. H., Gur, R. C., Emanuel, B. S., and Gur, R. E. (2017). White matter microstructural deficits in 22q11.2 deletion syndrome. *Psychiatry Res. Neuroimaging*, 268(March):35–44. doi: 10.1016/j.pscychresns.2017.08.001.

Scariati, E., Padula, M. C., Schaer, M., and Eliez, S. (2016). Long-range dysconnectivity in frontal and midline structures is associated to psychosis in 22q11.2 deletion syndrome. *J. Neural Transm.* doi: 10.1007/s00702-016-1548-z.

Schneider, M., Debbané, M., Bassett, A. S., Chow, E. W. C., Fung, W. L. A., van den Bree, M. B. M., Owen, M., Murphy, K. C., Niarchou, M., Kates, W. R., Antshel, K. M., Fremont, W., McDonald-McGinn, D. M., Gur, R. E., Zackai, E. H., Vorstman, J., Duijff, S. N., Klaassen, P. W. J., Swillen, A., Gothelf, D., Green, T., Weizman, A., Van Amelsvoort, T., Evers, L., Boot, E., Shashi, V., Hooper, S. R., Bearden, C. E., Jalbrzikowski, M., Armando, M., Vicari, S., Murphy, D. G., Ousley, O., Campbell, L. E., Simon, T. J., and Eliez, S. (2014). Psychiatric Disorders From Childhood to Adulthood in 22q11.2 Deletion Syndrome: Results From the International Consortium on Brain and Behavior in 22q11.2 Deletion Syndrome. *Am. J. Psychiatry*, 171(6):627–639. doi: 10.1176/appi.ajp.2013.13070864.

Schreiner, M. J., Karlsgodt, K. H., Uddin, L. Q., Chow, C., Congdon, E., Jalbrzikowski, M., and Bearden, C. E. (2014). Default mode network connectivity and reciprocal social behavior in 22q11.2 deletion syndrome. *Soc. Cogn. Affect. Neurosci.*, 9(9):1261–1267. doi: 10.1093/scan/nst114.

Smith, R. E., Tournier, J. D., Calamante, F., and Connelly, A. (2013). SIFT: Spherical-deconvolution informed filtering of tractograms. *Neuroimage*, 67:298–312. doi: 10.1016/j.neuroimage.2012.11.049.

Tang, E. and Bassett, D. S. (2018). Colloquium: Control of dynamics in brain networks. *Rev. Mod. Phys.*, 90(3):1–20. doi: 10.1103/RevModPhys.90.031003.

Tang, E., Giusti, C., Baum, G. L., Gu, S., Pollock, E., Kahn, A. E., Roalf, D. R., Moore, T. M., Ruparel, K., Gur, R. C., Gur, R. E., Satterthwaite, T. D., and Bassett, D. S. (2017). Developmental increases in white matter network controllability support a growing diversity of brain dynamics. *Nat. Commun.*, 8(1):1252. doi: 10.1038/s41467-017-01254-4.

Tournier, J. D., Calamante, F., and Connelly, A. (2007). Robust determination of the fibre orientation distribution in diffusion MRI: Non-negativity constrained super-resolved spherical deconvolution. *Neuroimage*, 35(4):1459–1472. doi: 10.1016/j.neuroimage.2007.02.016.

Tournier, J. D., Calamante, F., and Connelly, A. (2013). Determination of the appropriate b value and number of gradient directions for high-angular-resolution diffusion-weighted imaging. *NMR Biomed.*, 26(12):1775–1786. doi: 10.1002/nbm.3017.

Tournier, J. D., Smith, R. E., Raffelt, D. A., Tabbara, R., Dhollander, T., Pietsch, M., Christiaens, D., Jeurissen, B., Yeh, C.-H., and Connelly, A. (2019). MRtrix3: A fast, flexible and open software framework for medical image processing and visualisation. *bioRxiv Prepr.*, 551739. doi: 10.1101/551739.

Tylee, D. S., Kikinis, Z., Quinn, T. P., Antshel, K. M., Fremont, W., Tahir, M. A., Zhu, A., Gong, X., Glatt, S. J., Coman, I. L., Shenton, M. E., Kates, W. R., and Makris, N. (2017). Machine-learning classification of 22q11.2 deletion syndrome: A diffusion tensor imaging study. *NeuroImage Clin.*, 15(March):832–842. doi: 10.1016/j.nicl.2017.04.029.

Van Den Heuvel, M. P. and Fornito, A. (2014). Brain networks in schizophrenia. *Neuropsychol. Rev.*, 24(1):32–48. doi: 10.1007/s11065-014-9248-7.

Váša, F., Griffa, A., Scariati, E., Schaer, M., Urben, S., Eliez, S., and Hagmann, P. (2016). An affected core drives network integration deficits of the structural connectome in 22q11.2 deletion syndrome. *NeuroImage Clin.*, 10:239–249. doi: 10.1016/j.nicl.2015.11.017.

Wechsler, D. (1991). Weschler intelligence scale for children. *San Antonio, TX Psychol. Corp.*

Wechsler, D. (1997). Wechsler intelligence scale for adults. *London Psychol. Corp.*

Wu-Yan, E., Betzel, R. F., Tang, E., Gu, S., Pasqualetti, F., and Bassett, D. S. (2018). Benchmarking Measures of Network Controllability on Canonical Graph Models. *J. Nonlinear Sci.*, pages 1–39. doi: 10.1007/s00332-018-9448-z.

Yan Chaogan, Z. Y. (2010). DPARSF: a MATLAB toolbox for "pipeline" data analysis of resting-state fMRI. *Front. Syst. Neurosci.*, 4:13. doi: 10.3389/fnsys.2010.00013.

Zhan, L., Jenkins, L. M., Zhang, A., Conte, G., Forbes, A., Harvey, D., Angkustsiri, K., Goodrich-Hunsaker, N. J., Durdle, C., Lee, A., Schumann, C., Carmichael, O., Kalish, K., Leow, A. D., and Simon, T. J. (2018). Baseline connectome modular abnormalities in the childhood phase of a longitudinal study on individuals with chromosome 22q11.2 deletion syndrome. *Hum. Brain Mapp.*, 39(1):232–248. doi: 10.1002/hbm.23838.

Zöller, D., Schaer, M., Scariati, E., Padula, M. C., Eliez, S., and Ville, D. V. D. (2017). Disentangling resting-state BOLD variability and PCC functional connectivity in 22q11.2 deletion syndrome. *Neuroimage*, 149:85–97. doi: 10.1016/j.neuroimage.2017.01.064.

Zöller, D., Padula, M. C., Sandini, C., Schneider, M., Scariati, E., Van De Ville, D., Schaer, M., and Eliez, S. (2018). Psychotic symptoms influence the development of anterior cingulate BOLD variability in 22q11.2 deletion syndrome. *Schizophr. Res.*, 193:319–328. doi: 10.1016/j.schres.2017.08.003.

Zöller, D., Sandini, C., Karahanoğlu, F. I., Padula, M. C., Schaer, M., Eliez, S., and Van De Ville, D. (2019b). Large-scale brain network dynamics provide a measure of psychosis and anxiety in 22q11.2 deletion syndrome. *Biol. Psychiatry Cogn. Neurosci. Neuroimaging*, in press. doi: 10.1016/j.bpsc.2019.04.004.

Zöller, D. M., Bolton, T. A., Karahanoglu, F. I., Eliez, S., Schaer, M., and Van De Ville, D. (2019a). Robust recovery of temporal overlap between network activity using transient-informed spatio-temporal regression. *IEEE Trans. Med. Imaging*, 38(1):291–302. doi: 10.1109/TMI.2018.2863944.